

This article was downloaded by:

On: 15 January 2011

Access details: *Access Details: Free Access*

Publisher *Taylor & Francis*

Informa Ltd Registered in England and Wales Registered Number: 1072954 Registered office: Mortimer House, 37-41 Mortimer Street, London W1T 3JH, UK



## Comments on Inorganic Chemistry

Publication details, including instructions for authors and subscription information:

<http://www.informaworld.com/smpp/title~content=t713455155>

### Effect of Lattice Dynamics on Intramolecular Electron-Transfer Rates in Mixed-Valence Complexes

David N. Hendrickson<sup>a</sup>; Seung M. Oh<sup>a</sup>; Teng-Yuan Dong<sup>a</sup>; Takeshi Kambara<sup>ab</sup>; Michelle J. Cohn<sup>a</sup>; Michael F. Moore<sup>a</sup>

<sup>a</sup> School of Chemical Sciences, University of Illinois, Urbana, Illinois <sup>b</sup> Department of Engineering Physics, The University of Electro-Communications, Chofu, Tokyo, Japan

**To cite this Article** Hendrickson, David N. , Oh, Seung M. , Dong, Teng-Yuan , Kambara, Takeshi , Cohn, Michelle J. and Moore, Michael F.(1985) 'Effect of Lattice Dynamics on Intramolecular Electron-Transfer Rates in Mixed-Valence Complexes', *Comments on Inorganic Chemistry*, 4: 6, 329 – 349

**To link to this Article:** DOI: 10.1080/02603598508072271

**URL:** <http://dx.doi.org/10.1080/02603598508072271>

PLEASE SCROLL DOWN FOR ARTICLE

Full terms and conditions of use: <http://www.informaworld.com/terms-and-conditions-of-access.pdf>

This article may be used for research, teaching and private study purposes. Any substantial or systematic reproduction, re-distribution, re-selling, loan or sub-licensing, systematic supply or distribution in any form to anyone is expressly forbidden.

The publisher does not give any warranty express or implied or make any representation that the contents will be complete or accurate or up to date. The accuracy of any instructions, formulae and drug doses should be independently verified with primary sources. The publisher shall not be liable for any loss, actions, claims, proceedings, demand or costs or damages whatsoever or howsoever caused arising directly or indirectly in connection with or arising out of the use of this material.

## Effect of Lattice Dynamics on Intramolecular Electron-Transfer Rates in Mixed-Valence Complexes

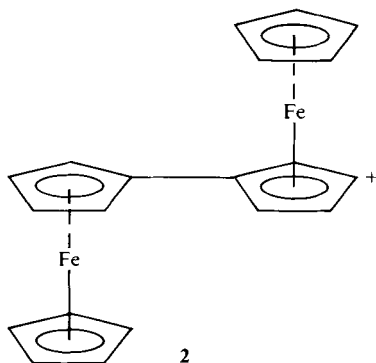
It is shown that the rates of intramolecular electron transfer for mixed-valence complexes in the solid state are not determined only by the electronic and vibronic coupling in the molecular complex. Lattice dynamics associated with the motion of ligands, solvate and counterions, which sometimes are manifested as phase transitions, frequently influence the electron-transfer rate.

### INTRODUCTION

It has been one and one-half decades since Taube<sup>1</sup> and Cowan<sup>2</sup> pioneered the use of mixed-valence transition metal complexes to probe electron transfer between well-separated metal sites. In these earliest studies, the Creutz-Taube ion (**1**) and the mixed-valence biferrocenium ion (**2**) were studied.



**1**



**2**

*Comments Inorg. Chem.*  
1985, Vol. 4, No. 6, pp. 329-349  
0260-3594/85/0406-0329/\$25.00/0

© 1985 Gordon and Breach,  
Science Publishers, Inc. and OPA Ltd.  
Printed in Great Britain

Studies of these two mixed-valence complexes are still under investigation.<sup>3–5</sup> The general goal has been to vary the bridge between the two metal centers and the solvent in order to understand the factors that control electron transfer between well-separated metal ions. It has always been assumed that two factors are the most important: (1) the electronic coupling between the d-manifolds on the two metal ions in the mixed-valence complex; and (2) the magnitude of vibronic coupling between the d-electrons and the molecular distortion. The PKS vibronic model<sup>6</sup> explicitly accounts for these two factors.

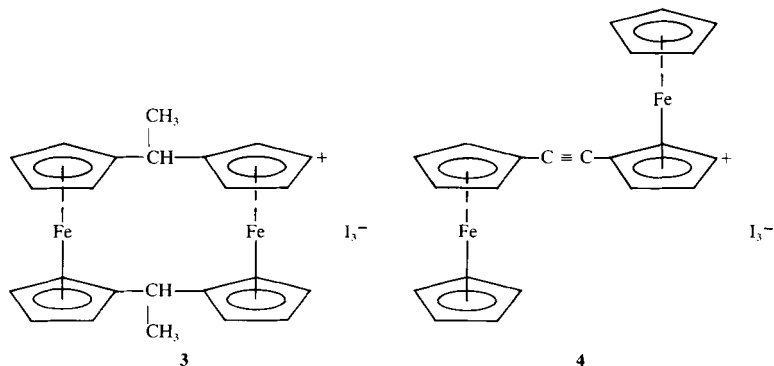
When mixed-valence complexes are studied in solution, the energy and band shape of the intervalence transfer (IT) electronic absorption band, generally seen in the NIR region, are used to characterize the degree of delocalization and the rate of thermal electron transfer. The simple Hush model<sup>7</sup> or the PKS vibronic model<sup>6</sup> can be used to analyze the IT band. The PKS model has been used to analyze the band shape of the IT bands seen for salts of **1**<sup>6</sup> and **2**.<sup>8</sup> The effects of the solvent are treated classically.

The measurement of the rate of thermal electron transfer for a mixed-valence complex *in the solid state* is carried out in a somewhat more direct manner. The different timescales of a battery of physical techniques are utilized.<sup>9,10</sup> In the past it has generally been assumed that the rate of intramolecular electron transfer in a given mixed-valence complex is *not* very much affected by the environment in the solid state. It is assumed that if there is no change in molecular conformation of the mixed-valence cation, there is little dependence of the rate on the counterion present in salts of species such as **1** or **2**. In this Comment it will be shown that the environment about a given mixed-valence complex can dramatically influence the rate of electron transfer. In the following sections some very recent results will be used to support this idea.

## MIXED-VALENCE BIFERROCENES

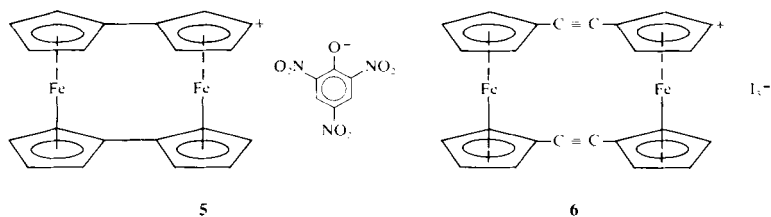
Until recently there were only two types of mixed-valence biferrocenes.<sup>9,11–15</sup> There are those that have relatively localized electronic structures, where the rate of intramolecular electron transfer in the solid state is less than the inverse of the <sup>57</sup>Fe Mössbauer timescale, i.e., the rate is less than  $\sim 10^7 \text{ s}^{-1}$ . This first type of

mixed-valence biferrocene salt gives a Mössbauer spectrum with two quadrupole-split doublets. One doublet is characteristic of a  $\text{Fe}^{\text{II}}$  metallocene and the other of a  $\text{Fe}^{\text{III}}$  metallocene. Compounds **3** and **4** are examples of such "localized" mixed-valence biferrocenes.



There is no x-ray structure available for **4**, but very recently the x-ray structure of **3** has been determined.<sup>16</sup> One metallocene moiety of the cation in **3** was found to be of the dimensions expected for a  $\text{Fe}^{\text{II}}$  metallocene, and the other is a  $\text{Fe}^{\text{III}}$  metallocene. It is important to note that in the solid state the  $\text{I}_3^-$  counterion is closer to the  $\text{Fe}^{\text{III}}$  ion than the  $\text{Fe}^{\text{II}}$  ion. The  $\text{Fe} \cdots \text{Fe}$  distance in the cation of **3** is 4.599(2) Å. In view of this short distance it is somewhat surprising that the intramolecular electron transfer is slower than  $\sim 10^7 \text{ s}^{-1}$  at 300 K. That is, with this short of a  $\text{Fe} \cdots \text{Fe}$  distance and if there is no influence on the potential-energy barrier from the environment, one might have expected a rate in excess of  $\sim 10^7 \text{ s}^{-1}$  from quantum mechanical tunneling.

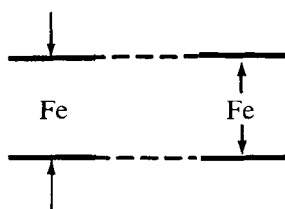
A completely delocalized electronic structure characterizes the second type of mixed-valence biferrocene. Compounds **5** and **6** exemplify this second type.



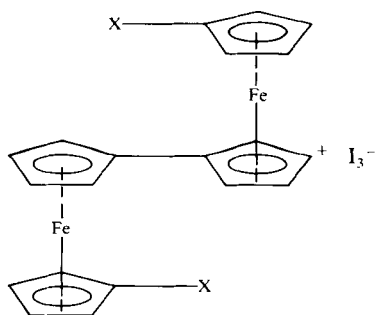
There is no x-ray structure available for **6**<sup>12</sup>; however, a structure has been reported<sup>17</sup> for the hemi-hydroquinone of **5**. The cation in **5** sits on a center of inversion; consequently, the two halves of this cation are crystallographically equivalent. The dimensions of each metallocene unit in **5** are intermediate between those of Fe<sup>II</sup> and Fe<sup>III</sup>. It is interesting that the cation in **5** is distorted with nonplanar fulvenide ligands and the two iron ions have moved together. The Fe...Fe distance [3.636(1) Å] in **5** is 0.35 Å shorter than the Fe...Fe distance in unoxidized bis(fulvalene)diiron. A single doublet is seen at all temperatures from 4.2 to 300 K in the Mössbauer spectra for various salts of the cation in **5**.<sup>9</sup> The same is true for **6**.<sup>12</sup> However, the most discriminating data for delocalized biferrocenes such as **5** and **6** are available from a simple IR experiment.<sup>12</sup> The perpendicular cyclopentadienyl C-H bending mode for a Fe<sup>II</sup> metallocene occurs in a range from 805 to 815 cm<sup>-1</sup>. The corresponding band for a Fe<sup>III</sup> metallocene is found in the range of 850 to 860 cm<sup>-1</sup>. The fact that complexes such as **5** and **6** have completely delocalized electronic structure is clearly indicated in the IR spectrum. For example, compound **6** gives a single cyclopentadienyl C-H bending band at 830 cm<sup>-1</sup>, a band that is intermediate in value between what is expected for Fe<sup>II</sup> and Fe<sup>III</sup> metallocenes. This indicates that there is no barrier for electron transfer in the cation of **6**. A relatively strong interaction between the appropriate d-orbitals on the two iron ions, an interaction propagated in **6** by the electron density of the two acetylene linkages, is present. The interaction is so strong that there is no potential-energy barrier for intramolecular electron transfer.

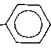
It is possible to generalize from the above observations. When either the Fe...Fe distance is small and a direct overlap of d orbitals is present or there are conjugated bridging groups that can propagate a strong electronic coupling between the two iron ions, there will be no barrier for electron transfer. The single unpaired electron has an equal probability of being on either half of the mixed-valence cation. This is probably the case for the cation in **5**. A mixed-valence complex could also develop a delocalized electronic ground state if both a moderate strength of electronic interaction between the two iron ions and a weak vibronic coupling between the d-electrons and the molecular distortion are present. Weak vibronic coupling ( $\lambda/k$ ) could result from two factors. Either the

vibronic coupling constant  $\lambda$  (refer to PKS theory<sup>6</sup> for explanation) could be small or the vibrational mode(s) that is (are) coupled to the electronic coordinates has (have) a large force constant. Perhaps the cation in **6** has a moderate electronic interaction and a large force constant for the vibrational mode coupled to the electronic coordinates. The large force constant could result from the two bridging moieties, the presence of which would lead to a strong interaction of the out-of-phase combination of ligand breathing modes of the two metallocene units in the cation, *viz.* (dashed lines are bridges):



When there is moderate or weak electronic coupling between the electronic manifolds of the two iron ions, there is then a potential-energy barrier for intramolecular electron transfer. In this case it is shown in this Comment that the static and dynamic nature of the environment in the solid state of such a mixed-valence species is the most important factor controlling the rate of intramolecular electron transfer. This can be established by summarizing some of our observations on the series **7**, a series of mixed-valence biferrocenes that has provided some rather enlightening data in the last few years.



- |                    |   |
|--------------------|---|
| <b>7a</b> , X = H  | <b>7e</b> , X = $-\text{CH}_2\text{CH}_3$   |
| <b>7b</b> , X = I  | <b>7f</b> , X = $-\text{CH}_2\text{CH}_2\text{CH}_3$  |
| <b>7c</b> , X = Br | <b>7g</b> , X = $-\text{CH}_2\text{CH}_2\text{CH}_2\text{CH}_3$   |
| <b>7d</b> , X = Cl | <b>7h</b> , X = $-\text{CH}_2-$  |

Single crystal x-ray structures have been determined for five of these eight compounds<sup>5,18–22</sup> and with known isostructural relationships between members of the series it can be said that the cations in all of the above compounds have a *trans* conformation in the solid state. The fulvenide ligand is planar in each cation and the iron ions are on opposite sides of the fulvenide ligand. The Fe···Fe distance is 5.1 Å for all cations in the series. Furthermore, it is likely that there is very little change in the *intramolecular* vibronic coupling (see Ref. 7 for a definition) of the mixed-valence cation across the series. There might be some *small* variation in electronic coupling from one cation to another, but as we will see, the variation in physical properties seen for the series **7** does *not* simply reflect any changes in electronegativity of the substituent X.

The cations in **7a**<sup>9</sup> and **7d**<sup>23</sup> undergo intramolecular electron transfer slower than the Mössbauer timescale ( $\sim 10^7$  s<sup>-1</sup>) in the range from 4.2 to 300 K. On the other hand, the cations in **7b**<sup>9</sup> and **7c**<sup>23</sup> transfer electrons faster than the Mössbauer timescale at 300 K. What is even more amazing is the fact that the cations in **7b** and **7c** also show only one “average-valence” doublet in their Mössbauer spectra at 4.2 K. Furthermore, the characteristics of the EPR spectra of **7b** and **7c** are appreciably different from those reported for localized species such as **7a**.<sup>9,24</sup> The EPR signals for **7b** and **7c** can be seen at room temperature, whereas much lower (<200 K) temperatures are needed to see the EPR spectrum of localized species. In addition, the g-tensors of the cations in **7b** and **7c** are considerably less anisotropic than that reported for the cation in **7a**. This seems to indicate that the intramolecular electron-transfer rates in **7b** and **7c** exceed the EPR timescale; that is, the rates are faster than  $\sim 10^{10}$  s<sup>-1</sup>. Very recent experiments,<sup>24</sup> however, have indicated that all eight of the cations in **7a–7h** are localized on the IR timescale. In the region of the cyclopentadienyl C-H bending modes (*vide supra*), each of the different cations shows one Fe<sup>II</sup> band and one Fe<sup>III</sup> band. The electron transfer is slower than  $\sim 10^{12}$  s<sup>-1</sup>.

Complexes **7e**,<sup>25</sup> **7f**,<sup>25</sup> **7g**,<sup>21</sup> and **7h**<sup>21</sup> exhibit a behavior that is different even from those described above for the complexes in series **7** that are either “valence-localized” or “valence-delocalized” on the Mössbauer timescale at 300 K. The four complexes **7e**, **7f**, **7g**, and **7h** give temperature-dependent Mössbauer spectra.

At temperatures below  $\sim 200$  K they each show two doublets, one for the  $\text{Fe}^{\text{II}}$  and the other for the  $\text{Fe}^{\text{III}}$  site. Increasing the sample temperature in each case leads to the two doublets moving together, eventually to become a single “average-valence” doublet at temperatures of 275, 245, 275, and 260 K, respectively. The temperature dependence of the Mössbauer spectrum for **7e** is shown in Fig. 1. There is one unusual feature that is quite evident in this figure. There is no line broadening evident at intermediate temperatures. The two doublets just move together with no line broadening to become a single average doublet. This is peculiar, for, if the electron transfer arises from thermal activation, in some temperature range the rate of electron transfer should go through the Mössbauer window. That is, the rate of transfer should become comparable to the inverse of the lifetime of the  $^{57}\text{Fe}$  nuclear excited state above some temperature and the lineshapes of the Mössbauer peaks would be affected. It appears that there are relaxation processes due to lattice dynamics occurring at a rate faster than can be sensed by the Mössbauer technique in the temperature range where the Mössbauer spectrum is changing.

With series **7** of mixed-valence compounds the rate of *intra*-molecular electron transfer ranges from less than  $\sim 10^7 \text{ s}^{-1}$  to greater than  $\sim 10^{10} \text{ s}^{-1}$ . With four of the compounds there is also an unusual Mössbauer temperature dependence seen. It is clear that the range in rates is *not* simply a manifestation of changes in the electronegativity of the X substituent. The  $\text{X} = \text{Cl}$  and  $\text{H}$  substituted compounds are localized on the Mössbauer timescale, whereas, the  $\text{X} = \text{I}$  and  $\text{Br}$  compounds are delocalized. We suggest that it is the environment about the mixed-valence cations in these compounds that is playing a major role in determining the rate of electron transfer. Very recent single-crystal x-ray structural results are in agreement with this view. The 298 K x-ray structure of the diiodo-substituted compound, **7b**, shows that the cation has the *trans* conformation with a mirror plane of symmetry going through the two iron and ring iodine atoms.<sup>18</sup> There is also a  $\text{C}_2$  axis perpendicular to this mirror plane and bisecting the central C-C bond of the necessarily planar fulvenide ligand. The two metallocene moieties in the cation are crystallographically equivalent. The natural consequence of this is that the  $\text{I}_3^-$  counterions are symmetrically disposed relative to the two iron ions in a given cation. The plot of potential energy versus reaction coordinate for electron



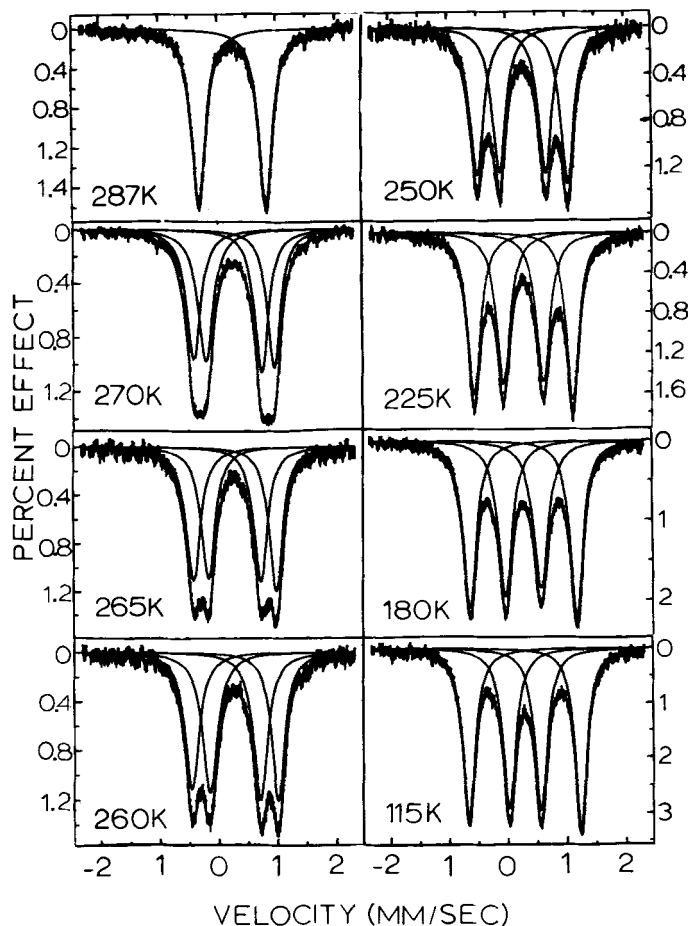


FIGURE 1 Variable-temperature  $^{57}\text{Fe}$  Mössbauer spectra for 1',6'-diethyl-biferrocenium triiodide, **7e**. The velocity scale is referenced to iron foil.

transfer is symmetric for this cation. There is a double-well potential with a barrier for electron transfer; however, intramolecular electron transfer is faster than  $\sim 10^{10} \text{ s}^{-1}$  in the range of 300 to 4.2 K.

On the other hand, the 298 K x-ray structure of **7d** shows that the  $\text{I}_3^-$  counterions are *not* symmetrically disposed relative to the

two iron ions in the mixed-valence cation.<sup>19</sup> Compound **7d** crystallizes with a half mole of  $I_2$ . In the solid state two  $I_3^-$  ions interact with the  $I_2$  molecule. When all the lattice forces are accounted for, the net result is that the environment about the cation in **7d** is *not* symmetric. The atoms in the  $I_3^-$  counterion are closer to one iron ion, the  $Fe^{III}$  ion, than to the other iron ( $Fe^{II}$ ). This asymmetric environment introduces asymmetry into the potential energy diagram. One minimum is at lower energy than the other in the double-well potential curve for the “ground-state surface” of this cation. The rate of intramolecular electron transfer is reduced considerably relative to the situation for the cation in **7b**, perhaps by three orders of magnitude.

The temperature dependence seen in the Mössbauer spectra of **7e**, **7f**, **7g**, and **7h** can also be explained in terms of the effects of the environment on the rate of electron transfer. The x-ray structures of **7f**<sup>20</sup> and **7g**<sup>21</sup> have been determined. The compound **7f** has been reported at 110 K to crystallize in  $P1$ , where the cation is asymmetric with  $Fe^{II}$  and  $Fe^{III}$  moieties. The atoms in the  $I_3^-$  anion are positioned closer to the  $Fe^{III}$  ion at this temperature. At 298 K **7f** has been reported to crystallize in  $P\bar{1}$ , where both the mixed-valence cation and the  $I_3^-$  anion are sitting on centers of symmetry. Obviously, at this higher temperature the  $I_3^-$  anion is symmetrically disposed relative to the two iron ions in the cation. It should be recognized that it is difficult to differentiate between  $P1$  and  $P\bar{1}$ . There is no differentiation possible based on differences in extinctions. Statistical tests can only *suggest* whether the centrosymmetric  $P\bar{1}$  case is present. The temperature dependence seen in the Mössbauer spectrum for **7f** can be explained by the following model. At low temperatures the  $I_3^-$  anions are sitting in fixed positions such that they are closer to  $Fe^{III}$  sites in nearby cations. When the temperature of **7f** is increased to some value, the  $I_3^-$  anions begin to move between two (or more) positions such that on the average they are symmetrically disposed relative to neighboring cations. This change in the disposition of the  $I_3^-$  anions from static to dynamic leads to a dramatic increase in the intramolecular electron-transfer rate in the mixed-valence cation. The potential energy diagram of the cation is changed as a result of the lattice dynamics. At low temperature there is an asymmetric double well and the cation is trapped in the lower energy state.

After the lattice dynamics set in, the double-well potential becomes symmetric.

There are actually two possibilities for the movement of the  $\text{I}_3^-$  anions in **7e**, **7f**, **7g**, and **7h**. As stated above, it is possible that the  $\text{I}_3^-$  anions move as a unit in the solid. However, it is more probable that the  $\text{I}_3^-$  anions are interconverting between two configurations, one which can be described in a limiting form as  $\text{I}_\text{A} \cdots \text{I}_\text{B} - \text{I}_\text{C}$  and the other one as  $\text{I}_\text{A} - \text{I}_\text{B} \cdots \text{I}_\text{C}$ . That is, in each configuration one I-I bond is shorter than the other one in each  $\text{I}_3^-$  anion. The thermal barrier for an  $\text{I}_3^-$  interconverting between two asymmetric configurations has been estimated<sup>26</sup> to be  $\sim 250 \text{ cm}^{-1}$ .

The absence of line broadening in the temperature evolution of the Mössbauer spectra of the dialkyl-substituted mixed-valence biferrocenes is explicable in terms of the above proposal. The averaging that is being seen in the Mössbauer spectra as the sample temperature is increased is the result of the lattice dynamics in the solid state. The lattice vibrations, i.e., phonons, that are activated when the  $\text{I}_3^-$  ions become dynamic are occurring at a frequency of  $\sim 10^{12} \text{ s}^{-1}$ . This is greatly in excess of rates that can be sensed by the  $^{57}\text{Fe}$  Mössbauer technique. It is now understandable why no line broadening is seen in the Mössbauer spectra.

If there are strong intermolecular interactions in the solid state between the mixed-valence cations, then the onset of the dynamics associated with the anion would be cooperative. A first-order phase transition would be seen. In this regard, it is interesting to note that we very recently found that biferrocenium triiodide shows an endothermic peak at  $\sim 334 \text{ K}$  in a differential scanning calorimetry scan.<sup>27</sup> The relatively narrow linewidth of this peak, combined with an observed hysteresis of  $\sim 2^\circ$  indicates that there is a first-order phase transition present. The results of the x-ray structure of biferrocenium triiodide, **7a**, clearly point to the presence of appreciable *intermolecular* interactions between cations.<sup>5</sup> There are slipped stacks of biferrocenium cations with cp–cp contacts between cations that are characterized by an interplanar distance of only  $3.44 \text{ \AA}$ . We have also found very recently that when **7a** is heated from  $300 \text{ K}$  the Mössbauer spectrum changes from one with two doublets to one with only one “average-valence” doublet at  $\sim 350 \text{ K}$ .<sup>5</sup> There appears to be a phase change present in biferrocenium triiodide.

Finally, a comment on the possibility of *intermolecular* electron transfer for mixed-valence biferrocenes in the solid state is in order. Variable-temperature (197–313 K) D.C. conductivity data have been reported<sup>28</sup> for powdered samples of **7a** and **7e**. At 300 K the conductivities of these two compounds are  $4.8 \times 10^{-6}$  and  $1.0 \times 10^{-5} \text{ S cm}^{-1}$ , respectively. It is not clear what these conductivities are attributable to; however, it is our feeling that the various phenomena reported above do *not* result from *intermolecular* electron transfer. It is true that there are appreciable intermolecular interactions between the mixed-valence cations in **7a**; however, the cations in **7g** do not have appreciable intermolecular cp–cp contacts. Also, the packing arrangement in **7b** consists of stacks, each of which are made up of an alternation of cations and anions. In this case the intermolecular electron transfer at 4.2 K would have to be propagated between cations via  $\text{I}_3^-$  anions. Furthermore, these compounds are stoichiometric mixed-valence compounds.

## TRINUCLEAR, MIXED-VALENCE IRON ACETATES

Mixed-valence trinuclear iron acetate complexes formally contain one  $\text{Fe}^{\text{II}}$  and two  $\text{Fe}^{\text{III}}$  ions and have the general structure shown in Fig. 2. In our studies the L ligand is pyridine(py) or a substituted pyridine. Several series of such complexes have been prepared, where in each series the composition of the trinuclear mixed-valence complex is *not* changed. In a given series the only difference between one compound and another is found in the solvate molecule. Two series are indicated below:

$[\text{Fe}_3\text{O}(\text{O}_2\text{CCH}_3)_6(\text{py})_3](\text{py})$	<b>8</b>
$[\text{Fe}_3\text{O}(\text{O}_2\text{CCH}_3)_6(\text{py})_3]$	<b>9</b>
$[\text{Fe}_3\text{O}(\text{O}_2\text{CCH}_3)_6(\text{py})_3](\text{benzene})$	<b>10</b>
$[\text{Fe}_3\text{O}(\text{O}_2\text{CCH}_3)_6(3\text{-CH}_3\text{-py})_3](3\text{-CH}_3\text{-py})$	<b>11</b>
$[\text{Fe}_3\text{O}(\text{O}_2\text{CCH}_3)_6(3\text{-CH}_3\text{-py})_3](\text{CH}_3\text{CN})_2$	<b>12</b>
$[\text{Fe}_3\text{O}(\text{O}_2\text{CCH}_3)_6(3\text{-CH}_3\text{-py})_3](\text{benzene})$	<b>13</b>
$[\text{Fe}_3\text{O}(\text{O}_2\text{CCH}_3)_6(3\text{-CH}_3\text{-py})_3](\text{toluene})$	<b>14</b>

The different compounds in one series are made by recrystallizing in the absence of oxygen the py or 3- $\text{CH}_3$ -py solvate in various

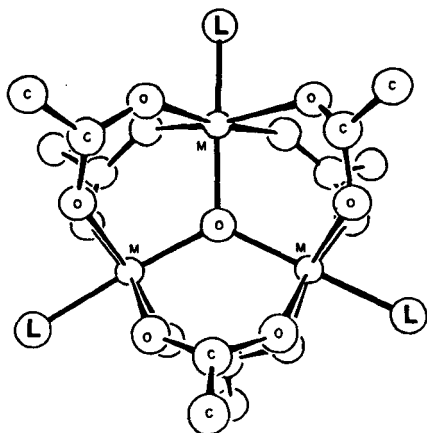


FIGURE 2 Molecular structure of trinuclear, oxo-centered, mixed-valence metal acetate complex.

solvents. There are now considerable data for these complexes. Brown *et al*<sup>29</sup> a few years ago first studied the temperature dependence of the Mössbauer spectra for the  $L = H_2O$  complex and for a poorly characterized version of the  $L = py$  compound.

Very recently several new and interesting observations have been made on the mixed-valence iron acetates. First, as we communicated recently,<sup>30</sup> it has been found that a change in the solvate molecule dramatically affects the rate of intramolecular electron transfer. In the first series above, for example, compound **9** gives a Mössbauer spectrum at liquid-nitrogen temperatures that is comprised of two doublets, one for high-spin  $Fe^{III}$  and the other for high-spin  $Fe^{II}$ . The  $Fe^{III} : Fe^{II}$  spectral area ratio is  $\sim 2.0$ . As the sample temperature is increased from liquid-nitrogen temperature to 315 K there is no evidence of electron transfer occurring. In contrast, there is a pronounced temperature dependence seen in the Mössbauer spectrum of compound **8** (see Fig. 3). At temperatures below  $\sim 110$  K two doublets are seen. As the sample temperature is increased from liquid-helium temperature, the first appreciable change in the spectrum is seen at  $\sim 112$  K, where a third doublet appears. The spectrum changes dramatically as the temperature is further increased, eventually to become a single doublet at temperatures above  $\sim 190$  K. It appears that the rate of *intra*-molecular electron transfer is increasing with increasing temper-

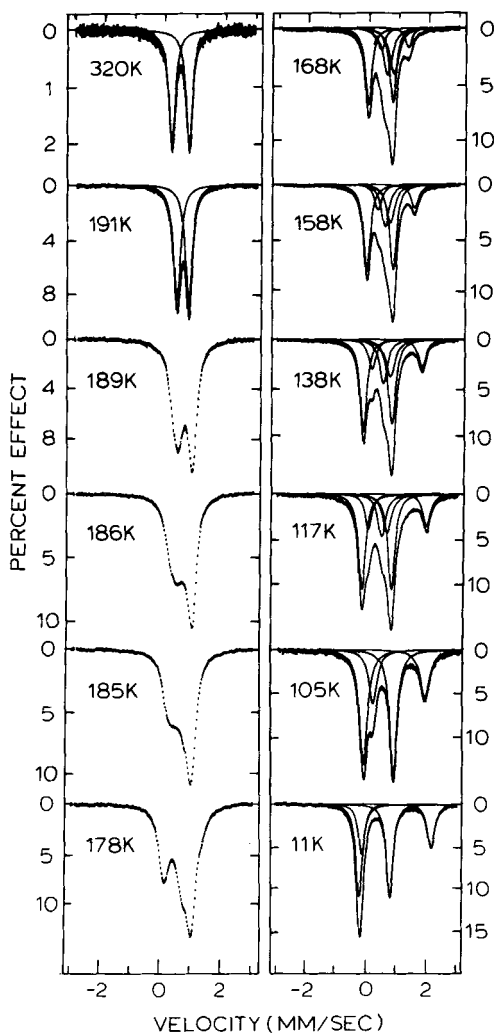


FIGURE 3 Variable-temperature  $^{57}\text{Fe}$  Mössbauer spectra for  $[\text{Fe}_3\text{O}(\text{O}_2\text{CC-H}_3)_6(\text{py})_3](\text{py})$ , **8**. The velocity scale is referenced to iron foil.

ature. Above  $\sim 190\text{ K}$  it exceeds the  $\sim 10^7\text{--}10^8\text{ s}^{-1}$  rate which the Mössbauer technique can sense.

As a second observation on mixed-valence iron acetates we have found that the triangular  $\text{Fe}_3\text{O}$  complex can undergo significant

dimensional changes as the sample temperature is changed. The x-ray structures of compound **11**<sup>31</sup> and of  $[\text{Fe}_3\text{O}(\text{O}_2\text{CCH}_3)_6(4\text{-Et-py})_3](4\text{-Et-py})$ ,<sup>30,32</sup> **15**, where 4-Et-py is 4-ethyl-pyridine, have been determined at room temperature and at a lower temperature (125 K for **11** and 163 K for **15**). In both cases the triangular complex becomes more equilateral as the crystal is heated from the low temperature to room temperature. For compound **15**, for example, there is a  $C_2$  axis through one iron ion ( $\text{Fe}^A$ ) and the oxide ion.<sup>30,32</sup> At low temperatures  $\text{Fe}^A$  must be the high-spin  $\text{Fe}^{\text{II}}$  ion and the two other iron ions ( $\text{Fe}^B$ ) are the high-spin  $\text{Fe}^{\text{III}}$  ions. At 163 K the bond distances to the central oxide ion are appreciably different:  $\text{Fe}^A\text{-O} = 2.010(4) \text{ \AA}$  and  $\text{Fe}^B\text{-O} = 1.856(7) \text{ \AA}$ . These two bond distances are closer to being equal in the 298 K structure:  $\text{Fe}^A\text{-O} = 1.953(5) \text{ \AA}$  and  $\text{Fe}^B\text{-O} = 1.879(2) \text{ \AA}$ . It is interesting that in going from 163 to 298 K the change in this bond length at the unique iron ion ( $\text{Fe}^A$ ) is negative and approximately twice as large [ $\Delta(\text{Fe}^A\text{-O}) = -0.057 \text{ \AA}$ ] as the positive change seen at the other two iron ions [ $\Delta(\text{Fe}^B\text{-O}) = +0.023 \text{ \AA}$ ].

A third general observation on mixed-valence iron acetates is that solvate molecules and/or pyridine ligands are found to be disordered in the x-ray structure determinations. The 4-Et-py ligand coordinated to the unique iron ion ( $\text{Fe}^A$ ) in compound **15** is seen to be disordered at 163 and 298 K. In fact, it has been suggested that this 4-Et-py ligand is statically disordered at low temperatures and begins to move between two positions above a certain temperature.<sup>30,32</sup> At 298 K the 4-Et-py ligand is dynamically disordered. Evidence for the presence of this dynamic disorder comes from the areas (recoilless fractions) of the two doublets seen for **15**. At temperatures below  $\sim 100 \text{ K}$  the area ratio of the two doublets is 2 : 1 ( $\text{Fe}^{\text{III}}$  :  $\text{Fe}^{\text{II}}$ ). As the sample temperature is increased above  $\sim 100 \text{ K}$ , the  $\text{Fe}^{\text{III}}$  :  $\text{Fe}^{\text{II}}$  area ratio increases until at 298 K it is 3.5 : 1. The dynamic disorder of the 4-Et-py ligand bonded to the  $\text{Fe}^A$  ion reduces the recoilless fraction of this iron site at high temperatures.

For **11**,<sup>31</sup> **8**<sup>31</sup> and  $[\text{Fe}_3\text{O}(\text{O}_2\text{CCH}_3)_6(4\text{-CH}_3\text{-py})_3](\text{C}_6\text{H}_6)$ ,<sup>31</sup> **16**, disorder has been found to be present in the solvate molecule. The packing arrangement in the 3- $\text{CH}_3$ -py compound **11** consists of stacks of  $\text{Fe}_3\text{O}(\text{O}_2\text{CCH}_3)_6(3\text{-CH}_3\text{-py})_3$  molecules. The disordered 3- $\text{CH}_3$ -py solvate molecules fill channels next to the stacks. In the case of **8** there are stacks of  $\text{Fe}_3\text{O}(\text{O}_2\text{CCH}_3)_6(\text{py})_3$  molecules with

the pyridine solvate molecules sandwiched between the molecules. The plane of the pyridine solvate molecule is parallel to the stacking direction and perpendicular to the planes of the  $\text{Fe}_3\text{O}$  moieties. At 298 K compound **8** crystallizes in R32.<sup>31,33</sup> The pyridine solvate molecule is disordered about the  $C_3$  axes that run down the stacks of  $\text{Fe}_3\text{O}$  complexes. In the temperature range of 300 down to 125 K compound **16** also crystallizes in R32 with the same basic stacked arrangement. The benzene solvate molecules are sandwiched between the  $\text{Fe}_3\text{O}$  complexes in each stack and are disordered about the  $C_3$  axis. As with the pyridine solvate molecules in the py compound, the planes of the benzene solvate molecules are perpendicular to the planes of the  $\text{Fe}_3\text{O}$  moieties in this 4- $\text{CH}_3$ -py compound.

The fourth general observation bearing on the issue of electron transfer in mixed-valence iron acetates can be gleaned from IR spectra<sup>34</sup> run for KBr-pellets of many of these compounds in the range of 250–4,000  $\text{cm}^{-1}$ . The  $\text{Fe}_3\text{O}$  asymmetric stretch regions ( $\sim 500\text{--}700\text{ cm}^{-1}$ ) of these compounds and analogous compounds are most revealing. The analogous  $\text{Fe}_3^{\text{III}}\text{O}$  complexes, such as  $[\text{Fe}_3\text{O}(\text{O}_2\text{CCH}_3)_6(4\text{-Et-py})_3]\text{ClO}_4$ , possess  $D_{3h}$  symmetry. As a result of this high symmetry, these  $\text{Fe}_3^{\text{III}}\text{O}$  complexes show *one*  $\text{Fe}_3\text{O}$  asymmetric stretching band. If the mixed-valence complexes become completely delocalized at room temperature, then they would also be expected to show but one  $\text{Fe}_3\text{O}$  asymmetric stretching band. However, we have found that complexes such as **15** exhibit two bands. Furthermore, the spectrum for this mixed-valence compound is quite similar to that obtained for  $[\text{Fe}_2^{\text{III}}\text{Co}^{\text{II}}\text{O}(\text{O}_2\text{CCH}_3)_6(4\text{-Et-py})_3](4\text{-Et-py})$ . It can be concluded that the mixed-valence iron acetates are localized on the infrared spectroscopy timescale. The rate of *intramolecular* electron transfer is less than  $\sim 10^{11}\text{ s}^{-1}$ . Finally, it should be mentioned that very little temperature dependence (down to 50 K) has been observed for the IR spectra of these complexes in the 400–4,000  $\text{cm}^{-1}$  region.

Most recently two other types of physical measurements have been carried out on the mixed-valence iron acetates. The results of these experiments will be described together with our proposal for the mechanism of intramolecular electron transfer in the solid state. It is our hypothesis that dynamics in the lattices of these mixed-valence iron acetates play an important role.<sup>30</sup> After all, the electronic “lability” of these mixed-valence complexes make



them very sensitive probes of the solid state. The environment about a mixed-valence  $\text{Fe}_3\text{O}$  complex in the solid state must either be symmetric or be able to adjust rapidly if the rate of intramolecular electron transfer is going to be appreciable. The complexes such as **9** and **12**, where we find no evidence for electron transfer in their Mössbauer spectra at room temperature, have either no solvate molecules present or small solvate molecules present. A compact lattice leaves little room for the adjustment in dimensions of the mixed-valence complex that would be needed to permit electron transfer. Our magnetic susceptibility experiments indicate that there is little difference between **8** and **9**.<sup>34</sup> Thus, the electronic interactions (i.e., magnetic exchange interactions) between the iron ions in **8** and **9** are of comparable magnitude. It must be the differences in solid state structure that lead to the different rates of electron transfer observed for **8** and **9**.

The heat capacity at constant pressure has very recently been determined for a 17.7794 g sample of **8** from 12 to 300 K.<sup>35</sup> There are two phase transitions present, a first-order phase transition with two  $C_p$  peaks at 111.4 and 112.0 K and a higher-order phase transition with two  $C_p$  peaks at 185.8 and 191.3 K. The higher-order phase transition evolves over a large temperature region, perhaps all the way down to  $\sim 113$  K. It is interesting that the temperatures of these two phase transitions and the large temperature range of the higher-order phase transition correspond well with changes seen in the Mössbauer spectrum of **8**. It is at  $\sim 112$  K where the first appreciable change in the spectrum is seen. A third "average-valence" type doublet appears at this temperature (see Fig. 3). Above 112 K the Mössbauer spectrum changes dramatically to become a single doublet above  $\sim 190$  K. The electron transfer process in **8** is intimately tied in with phase transitions in the solid state.

For compound **8** we suggest that the first-order phase transition at  $\sim 112$  K is an order-disorder phase transition.<sup>35(c)</sup> At temperatures below  $\sim 112$  K each of the mixed-valence  $\text{Fe}_3\text{O}$  complexes is valence localized. That is, each complex is distorted to reflect the valence description of  $\text{Fe}_2^{\text{III}}\text{Fe}^{\text{II}}\text{O}$ . Below  $\sim 112$  K these distorted complexes are ordered in domains, where within a given domain the sense of the distortion (i.e., which iron is  $\text{Fe}^{\text{II}}$ ) is the same for all the complexes in the domain. At  $\sim 112$  K these domains

disappear and there is first-order transition to a disordered state, which is characterized by a random distribution of the sense of distortion of the  $\text{Fe}_3\text{O}$  complexes. Examination of the packing diagram<sup>31</sup> for **8** clearly shows the nature of the intermolecular interaction that leads to this first-order phase transition, for, in addition to the stacking of  $\text{Fe}_3\text{O}$  complexes in **8**, there are also stacks of pyridine ligands. That is, the pyridine L ligands (see Fig. 2) of neighboring complexes are involved in appreciable  $\pi$ - $\pi$  overlaps. Furthermore, we suggest that concurrently with the order-disorder transformation there is, as a result of the change in the nature of intermolecular interactions, a change in the potential energy curve for the ground state of each  $\text{Fe}_3\text{O}$  complex. If the nondistorted configuration of the  $\text{Fe}_3\text{O}$  complex became equivalent in energy to the three distorted configurations of the  $\text{Fe}_3\text{O}$  complex, then this would explain the sudden appearance at  $\sim 112$  K of the third "average-valence" doublet in the Mössbauer spectrum of **8** (see Fig. 3).

The higher-order phase transition that evolves over a large temperature range and culminates in a peak at 191.3 K for **8** probably results from  $\text{Fe}_3\text{O}$  complexes becoming activated to transfer electrons. It is also very likely that this is influenced by the motion of the pyridine solvate molecule. The solvate molecules have their molecular planes aligned along the direction of the stacking and perpendicular to the planes of the  $\text{Fe}_3\text{O}$  moieties. Single-crystal x-ray results<sup>31</sup> indicate that there are  $C_3$  axes along the stacks of  $\text{Fe}_3\text{O}$  complexes. The pyridine solvate molecules are disordered in three positions to give this threefold symmetry. Preliminary x-ray diffraction results<sup>31</sup> also indicate that these  $C_3$  axes are absent below  $\sim 190$  K. This indicates that above  $\sim 190$  K the pyridine solvate molecules are moving rapidly between three equivalent positions, but that below  $\sim 190$  K these pyridine solvate molecules stop rotating about the  $C_3$  axes.

Clear evidence for motion of a solvate molecule in these trinuclear mixed-valence complexes has been obtained for  $[\text{Fe}_3\text{O}(\text{O}_2\text{CCH}_3)_6(4\text{-CH}_3\text{-py})_3](\text{C}_6\text{H}_6)$ , **16**. A sample of **16** where the benzene solvate is changed to  $\text{C}_6\text{D}_6$  has been prepared. Fixed-sample, spin-echo  $^2\text{H}$  NMR experiments have been performed on a single crystal of **16** at room temperature.<sup>35(a),36</sup> At every orientation of the single crystal a single quadrupole-split doublet is seen.

Thus, the  $C_6D_6$  molecules are rotating rapidly about pseudo sixfold axes such that there is only one deuteron site. But, even more importantly, it is found that the quadrupole moment interaction is reduced even more relative to a fixed  $C_6D_6$  molecule than would be expected for only the rotation about the pseudo sixfold axis. It is likely that these  $C_6D_6$  solvate molecules in **16** are rotating rapidly about the  $C_3$  axes running down the stacks.

For these trinuclear mixed-valence iron acetates it is clear that the rate of *intramolecular* electron transfer is very sensitively affected by the environment in which the  $Fe_3O$  complex is located. In certain cases it is possible to have motion in the solid state of the solvate molecules or even the pyridine ligands. These lattice dynamics dramatically influence the rate of electron transfer.

## GENERAL COMMENTS

From the above discussion it is clearly indicated that the environment about a binuclear or trinuclear mixed-valence complex can appreciably influence the rate of *intramolecular* electron transfer. Considerably more single-crystal x-ray diffraction, heat-capacity and solid-state NMR data are needed to understand in detail the full extent of this environmental control of electron transfer.

One can only wonder exactly what form this environmental control of electron-transfer rates takes for mixed-valence complexes in the solution state. The effect of solvent is well established. Ion pairing could also affect the rate of electron transfer for a mixed-valence complex that is charged. Also, just how rapidly does the solvent structure rearrange about such a mixed-valence complex in solution?

In biological electron-transport chains electron transfer occurs in many cases between two metal centers, each of which is buried in their separate protein structure. The distance between the two metal centers in nearby proteins can be very large, i.e., in excess of 15–20 Å. Electron transfer is believed to occur by quantum mechanical electron and/or nuclear tunneling between the two remote metal centers. Many of these metalloproteins in electron-transport chains are embedded or attached to membranes. The environment inside the metalloprotein is intermediate in nature

between the solid and solution states. It is quite possible that certain amino acid residues that make up a given "pathway" for electron transfer between two redox centers in nearby proteins or are in proximity to one redox center are involved in motion under physiological conditions. Obviously, the two nearby redox centers have very similar redox potentials, and, as a consequence, the motion of the amino acid residue could be modulating the rate of electron transfer. This is an environmental control of electron transfer that is similar to what is seen for the mixed-valence complexes in the solid state.

### Acknowledgments

We are grateful for funding from the National Institute of Health grant HL13652 and for our ongoing collaborations with Professors R. E. Davis, C. G. Pierpont, A. L. Rheingold, H. Sano, M. Sorai, C. E. Strouse and R. J. Wittebort.

DAVID N. HENDRICKSON,\* SEUNG M. OH,  
TENG-YUAN DONG, TAKESHI KAMBARA,†  
MICHELLE J. COHN and MICHAEL F. MOORE  
*School of Chemical Sciences,  
University of Illinois,  
Urbana, Illinois 61801*

### References

1. C. Creutz and H. Taube, *J. Am. Chem. Soc.* **92**, 3988 (1969).
2. D. O. Cowan and F. Kaufman, *J. Am. Chem. Soc.* **92**, 219 (1970).
3. For recent reviews of mixed-valence complexes see: (a) P. Day, *Int. Rev. Phys. Chem.* **1**, 149 (1981); (b) *Mixed-Valence Compounds, Theory and Applications in Chemistry, Physics, Geology, and Biology*, ed. D. B. Brown (Reidel, Boston, 1980); (c) C. Creutz, *Prog. Inorg. Chem.* **30**, 1 (1983); (d) D. E. Richardson and H. Taube, *Coord. Chem. Rev.* **60**, 107 (1984).
4. For recent work on **1** see: (a) U. Fűrholz, H. B. Bűrgi, F. E. Wagner, A. Stebler, J. H. Ammeter, R. J. H. Clark, M. Stead and A. Ludi, *J. Am. Chem.*

---

\* Author to whom correspondence should be sent.

† On sabbatical leave at University of Illinois. Permanent address: Department of Engineering Physics, The University of Electro-Communications, Chofu, Tokyo 182, Japan.

- Soc. **106**, 121 (1984); (b) E. Krausz and A. Ludi, *Inorg. Chem.* **24**, 939 (1985); (c) U. F rholz, S. Joss, H. B. B rger and A. Ludi, *Inorg. Chem.* **24**, 943 (1985).
5. The single-crystal x-ray structure of the  $I_3^-$  salt of **2** (compound **7a**) has been determined: M. J. Cohn, T.-Y. Dong, D. N. Hendrickson, S. J. Geib and A. L. Rheingold, *J. C. S. Chem. Commun.* (in press).
  6. K. Y. Wong and P. N. Schatz, *Prog. Inorg. Chem.* **28**, 369 (1981).
  7. (a) G. C. Allen and N. S. Hush, *Prog. Inorg. Chem.* **8**, 357 (1967); (b) N. S. Hush, *ibid.* **8**, 391 (1967).
  8. D. R. Talham and D. O. Cowan, *Organometallics* **3**, 1712 (1984).
  9. W. H. Morrison, Jr. and D. N. Hendrickson, *Inorg. Chem.* **14**, 2331 (1975).
  10. D. E. Richardson, *Comments Inorg. Chem.* **3**, 367 (1985).
  11. J. A. Kramer, F. H. Herbstein and D. N. Hendrickson, *J. Am. Chem. Soc.* **102**, 2293 (1980).
  12. J. A. Kramer and D. N. Hendrickson, *Inorg. Chem.* **19**, 3330 (1980).
  13. M. F. Moore and D. N. Hendrickson, *Inorg. Chem.* **24**, 1236 (1985).
  14. C. LeVanda, K. Bechgaard, D. O. Cowan, U. T. Mueller-Westerhoff, P. Eilbracht, G. A. Candela and R. L. Collins, *J. Am. Chem. Soc.* **98**, 3181 (1976).
  15. D. O. Cowan, P. Shu, F. L. Hedberg, M. Rossi and T. J. Kistenmacher, *J. Am. Chem. Soc.* **101**, 1304 (1979).
  16. A communication has appeared: M. F. Moore, S. R. Wilson, D. N. Hendrickson and U. T. Mueller-Westerhoff, *Inorg. Chem.* **23**, 2918 (1984); the full report is: M. F. Moore, S. R. Wilson, M. J. Cohn, T.-Y. Dong, U. T. Mueller-Westerhoff and D. N. Hendrickson (submitted for publication).
  17. M. Hillman and A. Kvik, *Organometallics* **2**, 1780 (1983).
  18. The single-crystal x-ray structure of **7b** has been determined: T.-Y. Dong, M. J. Cohn, D. N. Hendrickson and C. G. Pierpont, *J. Am. Chem. Soc.* (in press).
  19. The single-crystal x-ray structure of **7d** has been determined: T.-Y. Dong, D. N. Hendrickson and C. G. Pierpont (submitted for publication).
  20. M. Konno, S. Hyodo and S. Iijima, *Bull. Chem. Soc. Jpn.* **55**, 2327 (1982).
  21. The single-crystal x-ray structure of **7g** has been determined at 150, 298, and 363 K: T.-Y. Dong, D. H. Hendrickson, K. Iwai, M. J. Cohn, S. J. Geib, A. L. Rheingold, H. Sano, I. Motoyama and S. Nakashima (submitted for publication).
  22. The single-crystal x-ray structure of **7h** is in progress: C. G. Pierpont, T.-Y. Dong and D. N. Hendrickson.
  23. I. Motoyama, K. Suto, M. Katada and H. Sano, *Chem. Lett.* 1215 (1983).
  24. T.-Y. Dong and D. N. Hendrickson (unpublished results).
  25. S. Iijima, R. Saida, I. Motoyama and H. Sano, *Bull. Chem. Soc. Jpn.* **54**, 1375 (1981).
  26. R. D. Brown and E. K. Nunn, *Aust. J. Chem.* **19**, 1567 (1966).
  27. M. J. Cohn, T.-Y. Dong and D. N. Hendrickson (unpublished results).
  28. S. Iijima and Y. Tanaka, *J. Organometallic Chem.* **270**, C11–C14 (1984).
  29. C. T. Dziobkowski, J. T. Wroblewski and D. B. Brown, *Inorg. Chem.* **20**, 679 (1981).
  30. S. M. Oh, D. N. Hendrickson, K. L. Hassett and R. E. Davis, *J. Am. Chem. Soc.* **106**, 7984 (1984).
  31. S. M. Oh, D. N. Hendrickson and C. E. Strouse (unpublished results).
  32. S. M. Oh, D. N. Hendrickson, K. L. Hassett and R. E. Davis (submitted for publication).
  33. Compound **8** is isostructural with  $[Mn_3O(O_2CCH_3)_6(py)_3](py)$ , the structure of

- which has been communicated: A. R. E. Baikie, M. B. Hursthouse, D. B. New and P. Thornton, *J. Chem. Soc. Chem. Commun.* 62 (1978).
34. S. M. Oh and D. N. Hendrickson (unpublished results).
  35. (a) S. M. Oh, T. Kambara, D. N. Hendrickson, M. Sorai, K. Kaji and R. J. Wittebort (submitted for publication); (b) M. Sorai, K. Kaji, S. M. Oh and D. N. Hendrickson (manuscript in preparation); (c) T. Kambara, M. Sorai, S. M. Oh and D. N. Hendrickson (manuscript in preparation).
  36. R. J. Wittebort, S. M. Oh and D. N. Hendrickson (manuscript in preparation).